Supplementary Information Appendix

Adrian Jacobo and A. J. Hudspeth

Howard Hughes Medical Institute and Laboratory of Sensory Neuroscience

The Rockefeller University, New York, NY 10065-6399, USA

Corresponding Author: A. J. Hudspeth

Howard Hughes Medical Institute and Laboratory of Sensory Neuroscience

The Rockefeller University, New York, NY 10065-6399, USA

Telephone: 212 327 735

E-mail: hudspaj@rockefeller.edu

S.1 Modeling the morphogens

The reactions for our model [1] are:

$$A \underset{k_{-1}}{\overset{k_1}{\rightleftharpoons}} U, \qquad B \overset{k_2}{\to} V, \qquad 2U + V \overset{k_3}{\to} 3U. \tag{S1}$$

We first consider that the concentrations of A and B are kept constant and homogeneous in the system and that U and V are diffusible molecules. Using the law of mass action, we can then write a system of equations for the time evolution of the concentrations of U and V:

$$\begin{aligned} \frac{\partial u}{\partial t} &= k_1 a - k_{-1} u + k_3\ u^2 v + d_u \nabla^2 u, \\ \frac{\partial v}{\partial t} &= k_2 b - k_3\ u^2 v + d_v \nabla^2 v. \end{aligned} \tag{S2}$$

in which a, b, u, and v are the concentrations of A, B, U, and V respectively and the k_i are the rate constants of each reaction. d_u and d_v are the diffusion coefficients of U and V. Because the process of morphogenesis occurs at the apical surface of the cell [2], we solve these equations in a unit disc $D = \{x, y \mid x^2 + y^2 \leq 1\}$. In cartesian coordinates $\nabla^2 = \partial^2/\partial x^2 + \partial^2/\partial y^2$ and the boundary conditions are

$$(\boldsymbol{n} \cdot \nabla) \begin{pmatrix} u \\ v \end{pmatrix} = 0 \text{ on } \partial B$$

in which $\partial B = \{x, y \mid x^2 + y^2 = 1\}$ is the closed boundary of B and $\boldsymbol{n}$ is the unit outward normal to ∂B.

To nondimensionalize the system we now consider the following change of variables

$$
\begin{aligned}
u' &= u\left(\frac{k_3}{k_{-1}}\right)^{\frac{1}{2}}, & v' &= v\left(\frac{k_3}{k_{-1}}\right)^{\frac{1}{2}}, & t' &= \frac{t}{\tau},\\
a' &= a\frac{k_1}{k_{-1}}\left(\frac{k_3}{k_{-1}}\right)^{\frac{1}{2}}, & b' &= b\frac{k_2}{k_{-1}}\left(\frac{k_3}{k_{-1}}\right)^{\frac{1}{2}}, & x' &= \frac{x}{L},\\
d'_u &= \frac{d_u}{L^2}\tau, & d'_v &= \frac{d_v}{L^2}\tau, & \gamma &= k_{-1}\tau,
\end{aligned}
$$

in which L and τ are characteristic length and time scales of the system. Inserting these new variables in Eqs. (S2) and dropping the primes for convenience we obtain:

$$
\begin{aligned}
\frac{\partial u}{\partial t} &= \gamma(a - u + u^2 v) + d_u \nabla^2 u,\\
\frac{\partial v}{\partial t} &= \gamma(b - u^2 v) + d_v \nabla^2 v.
\end{aligned}
\tag{S3}
$$

Here u, b, a, and v are now the dimensionless concentrations of their respective chemical species.

S.1.1 Linear stability analysis

The rescaling introduced above is used in the main text and simulations because it allows us to independently control the spatial scale of the system by changing the diffusion constants. This control facilitates fitting the solutions of Eqs. (S3) to the dimensions and characteristics of actual hair bundles. In order to calculate the stability of the system we now introduce an additional rescaling to simplify algebraic calculations. We consider the following change of variables:

$$d = \frac{d_v}{d_u},\ \gamma' = \frac{\gamma}{d_u},\ t' = d_u t.$$

Then, after dropping the primes, Eqs. (S3) become

$$\begin{aligned} \frac{\partial u}{\partial t} &= \gamma(a - u + u^2 v) + \nabla^2 u, \\ \frac{\partial v}{\partial t} &= \gamma(b - u^2 v) + d\,\nabla^2 v. \end{aligned} \tag{S4}$$

Because we are interested in the instabilities that can occur regardless of boundary effects, we consider an infinite system. We calculate the homogeneous steady state of the system by setting the spatial and temporal derivatives to zero to obtain

$$u_0 = a + b,\ v_0 = \frac{b}{(a+b)^2}. \tag{S5}$$

For this solution to become unstable and develop patterns the following conditions must be met [3]:

$$0 < b - a < (a+b)^3, \tag{S6}$$

$$(a+b)^2 > 0, \tag{S7}$$

$$d(b-a) > (a+b)^3, \tag{S8}$$

$$[d(b-a) - (a+b)^3]^2 > 4d(a+b)^4. \tag{S9}$$

Inequalities (S6) and (S7) specify the conditions for the homogeneous steady-state so-

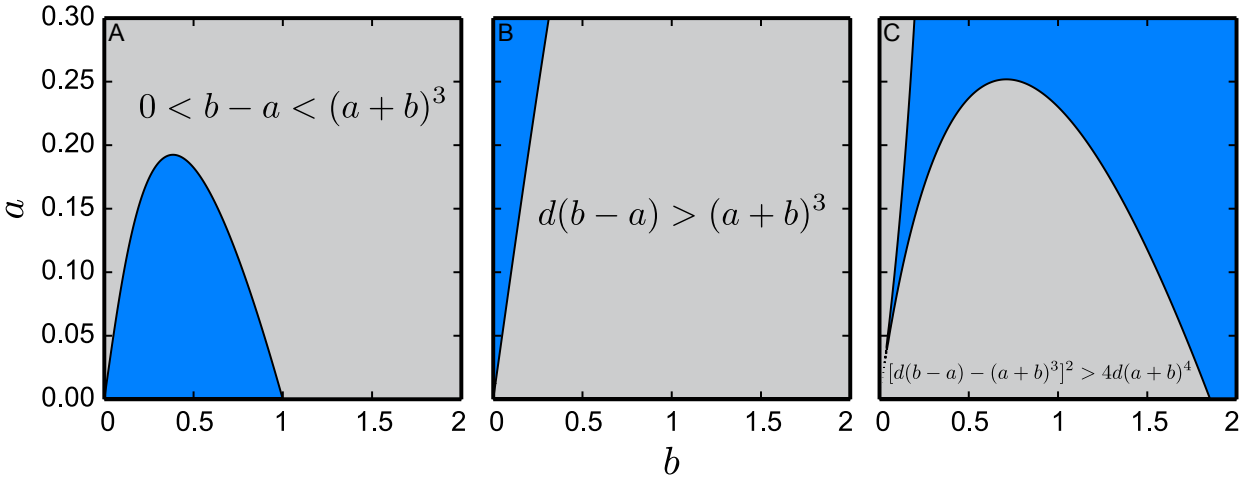

Figure S1: Linear stability analysis of the system. The system has a Turing instability when Ineqs. (S6)-(S9) are fullfiled simultaneously. Gray areas indicate the region of validity of each inequality. A) When Ineq. (S6) is violated (blue area) the system has a Hopf bifurcation which produces homogeneous oscillatory solutions. B) Ineq. (S8), C) Ineq. (S9)

lution (S5) to be stable. Inequality (S6) implies that $b > a$. When it is violated the homogeneous steady-state solution becomes unstable through a Hopf bifurcation (Fig. S1A). Inequality (S7) is trivial.

Inequality (S8) combined with (S6) require that the ratio of diffusion coefficients $d > 1$. This implies that V must diffuse faster than U for patterns to form. Finally, combining inequalities (S6), (S8), and (S9) (Fig. S1) we obtain the region of Turing instability (Fig. 2A in the main text).

To study the shape of hair bundles as a function of the substrate gradients, integrating Eqs. (S3) is computationally intensive and time consuming. A much faster approach is to use Inequalities (S6)-(S9) to find the area of the cell where a hexagonal pattern can develop, setting the area of the bundle. To do this we apply these inequalities to the values of a and b at each point on the cell's surface. Points where the inequalities are fulfilled are unstable to the formation of the pattern and therefore are part of the bundle. Because Inequalities

(S6)-(S9) were derived considering homogeneous concentrations of the substrates instead of gradients, the regions of pattern formation reconstructed by this method are approximations. By comparing the edges of the bundles obtained with this method with those obtained by solving Eqs. (S3) we find that this approximation works well enough to determine the overall shape of hair bundles in a time-efficient way.

S.2 Modeling the substrates

We assume that the substrates A and B are produced at their respective sources, transported by diffusion, and decay at constant rates. This process is described by

$$\begin{aligned} \frac{\partial a}{\partial t} &= d_a \nabla^2 a - k_a a, \\ \frac{\partial b}{\partial t} &= d_b \nabla^2 b - k_b b, \end{aligned} \tag{S10}$$

in which d_a and d_b are the respective diffusion constants of the substrates and k_a and k_b their decay rates. These equations are nondimensionalized similarly to Eqs. (S3). As for the morphogens we assume that the diffusion terms are two-dimensional and we use reflecting boundary conditions unless stated otherwise. A and B have sources with shapes $S_a(x, y)$ and $S_b(x, y)$. At each of these sources the values of a and b are fixed to a_0 and b_0 respectively. When one of the sources its located at the edge of the cell it therefore replaces the reflecting boundary condition for the corresponding substrate. If the source is placed at the kinocilium then it acts as an internal boundary condition, fixing the value of the field at a particular point. Although in principle Eqs. (S11) should include the terms $-\gamma a$ and $-\gamma b$ reciprocal to those in Eqs. (S3), these terms can be eliminated by redefining k_a and k_b.

We assume that the substrates evolve on a much faster timescale than the morphogens.

We can accordingly use adiabatic elimination of a and b and treat them as constant in time, eliminating the temporal derivatives in Eqs. (S11) to obtain

$$d_a \nabla^2 a - a = 0, \tag{S11}$$
$$d_b \nabla^2 b - b = 0,$$

in which we redefined $d_a = d_a/k_a$ and $d_b = d_b/k_b$. These relations show that the stationary shapes of the substrate gradients depend only on the diffusion parameters d_a and d_b and on the concentrations a_0 and b_0 at their sources.

S.2.1 Location of the sources

In our model we locate the source of A at the boundary of the cell and the source of B at the kinocilium. Although the choice of these two sources makes sense from the morphology of hair cells and the available experimental evidence, there are different options to be considered in deciding which substrate corresponds to each source.

The first option to consider is whether in fact two substrates are needed or similar results could be obtained with only one. A substrate gradient acts as a ruler: the decrease in concentration with distance from a source can be used to measure the position relative to it. If there were only one substrate involved in the process of morphogenesis, the edge of the hair bundle could assume only the shape of the isoconcentration lines of that substrate; it would be impossible to reproduce the observed shape of a hair bundle. Following this same, argument it is easy to see that having two substrates with sources located at the boundary of the cell could produce only bundles with radial symmetry, excluding this possibility as well.

The next possibility is for both A and B to have sources at the kinocilium. In this case

the reflecting boundary conditions at the edge of the cell break the rotational symmetry around the kinocilium, allowing for bundle shapes with this broken symmetry (Fig. S2). Even in this case, the clustered stereocilia always surround the kinocilium, including some in the narrow space between the kinocilium and the edge of the cell. This configuration is also unable to produce bundles that are confined to the center of the cell, without touching its boundary, and is therefore unable to reproduce the observed shape of normal bundles.

A final issue is the possibility of interchanging the sources of the substrates, using the kinocilium as the source of A and the edge of the cell as the source of B (Fig. S3). In this configuration the system produces bundles with morphologies similar to actual bundles, but with a correlation between the size of the bundle and the position of the kinocilium: the smaller the area of the bundle, the farther it lies from the kinocilium. This correlation makes it impossible to find a set of parameter values that fits the shape of actual bundles, for bundles of the right size appear disconnected from the kinocilium.

We can therefore see that a minimum of two substrates is needed to obtain the observed shapes of the bundle and, if we consider the pattern-formation dynamics given by Eqs. (3), the only option for the sources that can fit the observed shape of hair bundles places the boundary of the cell as the source of A and the kinocilium as the source of B.

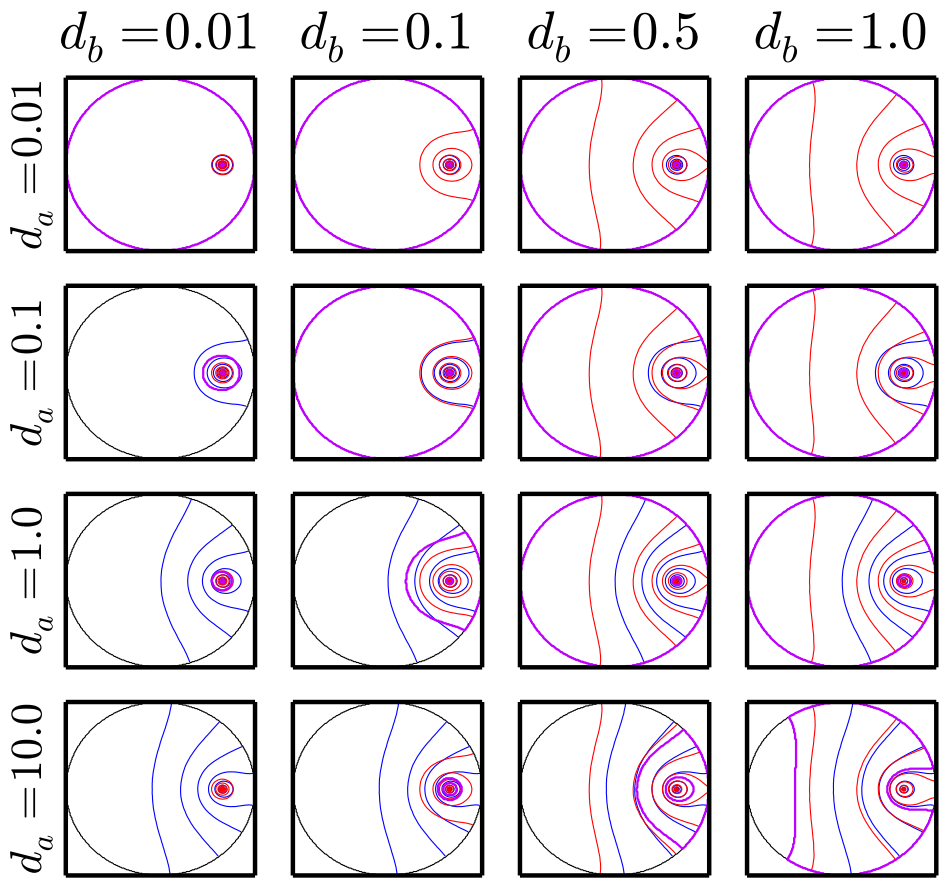

Figure S2: Isoconcentration lines for the substrates A (blue) and B (red) and approximated shapes of the predicted hair bundles (purple) as a function of the parameter values. In this case, the source of both substrates is located at the kinocilium. $a_0 = 0.28$ and $b_0 = 2$.

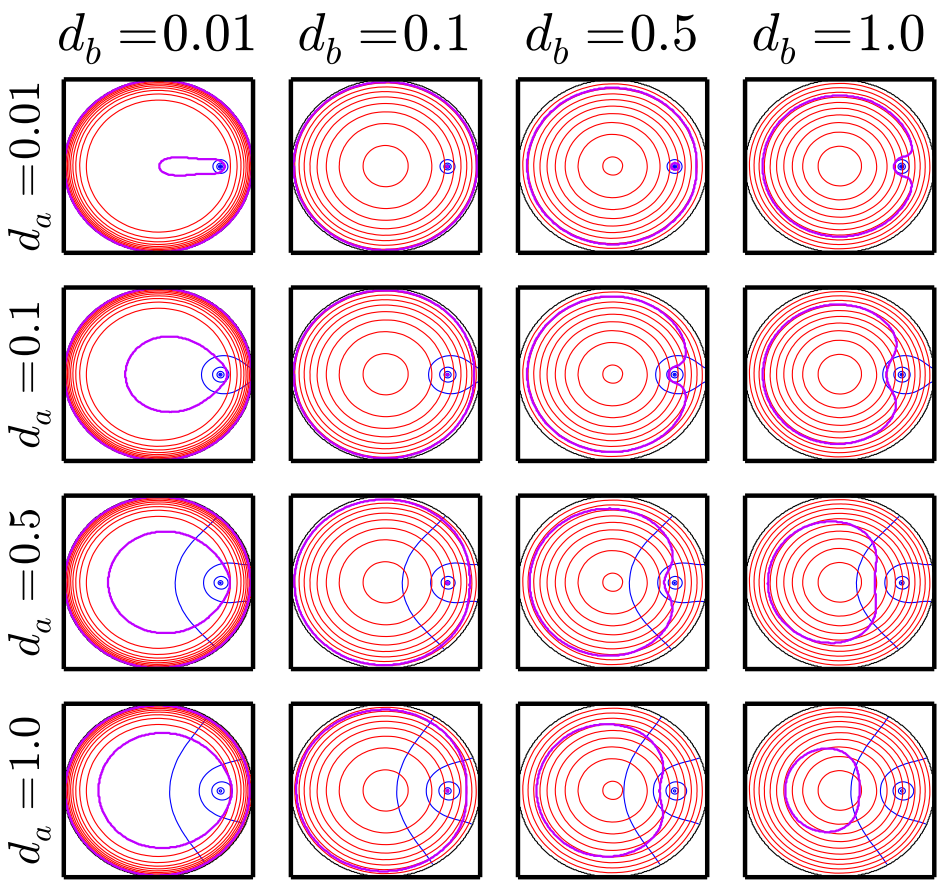

Figure S3: Isoconcentration lines for the substrates A (blue) and B (red) and approximated shapes of the predicted hair bundles (purple) as a function of the parameter values. The source of A is located at the kinocilium and the source of B is located at the edge of the cell. $a_0 = 0.28$ and $b_0 = 2$.

References

[1] Schnakenberg, J. (1979) Simple chemical reaction systems with limit cycle behaviour *J Theoret Biol* 81:389-400

[2] Ezan, J. et al. (2013) Primary cilium migration depends on G-protein signalling control of subapical cytoskeleton. *Nat Cell Biol* 15:1107-15.

[3] Murray, J. J. (2003) *Mathematical Biology. II: Spatial Models and Biomedical Applications* (Springer-Verlag, New York), 3rd edition.